Morphological instability of crystal growth in nonsteady potentiostatic electrodeposition. II. Experimental examination with the image analysis of crystal morphology

Ryoichi Aogaki and Tohru Makino

Citation: The Journal of Chemical Physics **81**, 2164 (1984); doi: 10.1063/1.447841
View online: http://dx.doi.org/10.1063/1.447841
View Table of Contents: http://scitation.aip.org/content/aip/journal/jcp/81/4?ver=pdfcov
Published by the AIP Publishing

Morphological instability of crystal growth in nonsteady potentiostatic electrodeposition. II. Experimental examination with the image analysis of crystal morphology

Ryoichi Aogaki and Tohru Makino[a)]
Department of Chemistry, The Institute of Vocational Training, 1960, Aihara, Sagamihara, 229, Japan

(Received 19 November 1982; accepted 6 March 1984)

In the accompanying paper, a theoretical equation governing unstable crystal growth under a nonsteady potentiostatic condition was derived. In the present paper, in order to examine the theory with experiments, the electrodeposition of Ag crystals on Ag electrodes was performed. SEM photographs of the Ag samples deposited during various periods of time were immediately taken for analyzing them by the technique of image analysis. As a result, it was found that the mean crystal size-deposition time curve can be calculated by means of the theory. It was then concluded that the surface diffusion coefficient takes a value in good agreement with the theoretical prediction, and that the surface energy of the electrode depends on the overpotential, i.e., it decreases with increasing overpotential, after passing about -0.2 V, however, the value becomes constant.

I. INTRODUCTION

As shown in the accompanying paper, in potentiostatic deposition, the effect of the surface diffusion of adatoms is very important in the region of high cathodic polarization. However, surface diffusion in electrodeposition has been discussed by only few people, e.g., Bockris *et al.*,[1–4] Gerisher,[5] and Lorenz.[6] They applied a constant or alternating current to the metal deposition system, then analyzed its nonsteady response.

In spite of previous efforts, this effect itself has not been made clear so far. For this reason, a direct process was proposed[7] where deposition without any surface diffusion of adatoms takes place directly at active sites on the electrode surface. Consequently, as for the important parameters of the surface diffusion, only equilibrium adatom concentrations were measured for several metals while the surface diffusion coefficient has not hitherto been obtained. Moreover, the surface energy of an electrode, especially that of an active electrode which itself takes part in the electrode reaction, has not so far been reported. Nevertheless, from measurements with thin metal foils, it has been known that the surface energy of an inactive electrode like Pt is largely dependent on the electrode potential in a manner similar to that represented by an electrocapillary curve for a liquid metal electrode system.[8]

Taking into consideration the results mentioned above, we attempted first of all to obtain experimental data for crystal particles formed during various deposition times. The surface parameters were then determined by curve fitting of computed results to the experimental data. From the theoretical calculation in terms of the parameters, the validity of the theory with respect to the time-dependence of crystal growth was examined.

II. EXPERIMENTS AND CALCULATIONS

Using 1 M $HClO_4$ as a supporting electrolyte, Ag deposition on Ag electrode in $AgClO_4$ solutions was carried out. The electrode was made of polycrystalline of Ag having a purity of 99.99%. Immediately after chemically polishing the surface, the electrode was prepared for the experiment by being rinsed with twice-distilled water.[9] All the chemicals were reagent grade, and the temperature of the solution was maintained at 300 K. The electrode cell configuration used was explained elsewhere.[14] Ag crystals were then deposited on the electrode during a given time under potentiostatic conditions. The sample was again rinsed with distilled water, and dried by flowing N_2 gas. After taking photographs of it by SEM, we measured the average size of the crystals on the electrode and their standard deviation by use of a Toyo Ink Luzex 500 Image Analyzer. The size of a crystal was defined as the diameter of the equivalent circle having the same area. All experiments were performed after confirming that the diffusion-limited behavior was obtained.

On the other hand, theoretical calculations to derive the crystal size distribution was carried out as described previously[10]; assuming a rectangular electrode surface with a given area which was divided into a grid of 128×128 points, random numbers generated by computer were assigned to each of the grid points. Interpolation between neighboring grid point data yielded a matrix with 256×256 data points. As a result of the procedure mentioned above, the initial fluctuation $\zeta(x, y, 0)$ of surface height arising from microscopic deposition and dissolution was established.

The fluctuation $\zeta(x, y, 0)$ comes from a thermodynamical equilibrium existing between adatoms on an electrode surface and metal ions in the solution near the surface. Immediately after superimposing a cathodic potential step to the surface, the electrode system transfers to nonequilibrium state, at the same time, nonsteady diffusion of the metal ions successively takes place. Then, the fluctuation grows up to macroscopic scale. Henceforth, the initial fluctuation was

[a)] Present address: AHS Japan Co., 2-10-12, Akasaka, Minato-ku, 107, Japan.

 0021-9606/84/162164-05$02.10

converted into a Fourier image function by means of a two-dimensional Fourier transform.[13] The image function of the initial fluctuation $Z(k_x,k_y,0)$ can then be represented as follows[9]:

$$Z(k_x,k_y,0) = 1/2\pi \int_{-\infty}^{\infty}\int_{-\infty}^{\infty} \zeta(x,y,0) \times \exp[-i(k_x x + k_y y)]\,dx\,dy, \quad (1)$$

(in the previous report,[9] 2π in Eqs. (1) and (4) of the present paper is written as $\sqrt{2\pi}$, which are misprints) where $i \equiv \sqrt{-1}$, and k_x and k_y are the x and y components of spatial wave number k, respectively. From the dsi (degree of surface irregularity) equation, developed in the previous paper (part I), the transfer function for potentiostatic deposition at a time t is defined as

$$F(k_x,k_y,t) = \exp\left\{\frac{\sigma\Omega D\{2RT\sqrt{t/\pi D}\,[C^*(z=\infty) - C^*(z=Z^*)]}{(nF)^2 DC^*(z=Z^*) + \sigma RT} - \frac{\Omega\gamma C^*(z=Z^*)tk^2\}k - D_{ad}C_{ad}^*\Omega^2\gamma t}{RT}k^4\right\}, \quad (2)$$

where $k \equiv (k_x^2 + k_y^2)^{1/2}$, and the notations for all the parameters in this paper are the same as used in part I.

Applying the transfer function to the image function, $Z(k_x,k_y,0)$ at $t = 0$, the image function $Z(k_x,k_y,t)$ at $t = t$ is represented as

$$Z(k_x,k_y,t) = Z(k_x,k_y,0)F(k_x,k_y,t). \quad (3)$$

Equation (3) depicts the process how the surface fluctuation develops with time from an equilibrium state to a nonequilibrium state in the Fourier image space. According to Eq. (3), the image function for nonequilibrium states can be calculated in terms of the transfer function essential to the electrode system and the image function for the equilibrium fluctuation.

Finally, the Fourier inversion of this function leads to the following equation which represents the three-dimensional surface morphology at $t = t$[9]:

$$\zeta(x,y,t) = 1/2\pi \int_{-\infty}^{\infty}\int_{-\infty}^{\infty} Z(k_x,k_y,t) \times \exp[i(k_x x + k_y y)]\,dk_x\,dk_y. \quad (4)$$

Using the root–mean–square height h_{rms} for the height distribution of the electrode, we regard the portions higher than h_{rms} as projecting parts for calculation, and in order to determine the theoretical average crystal size and its standard deviation, a statistical calculation for the protruding areas was carried out. The three-dimensional contour lines of the peaks were then plotted by use of the results of the calculation for $\zeta(x,y,t)$. The program for the plotting is the same as used for illustrating the surface morphology in the previous paper.[9] At the same time, cross-sectional profiles of the electrode surface were also plotted.

III. RESULTS AND DISCUSSION

Figures 1, 2, and 3 are examples of SEM photographs for the crystal morphology at different deposition times. As expected above, the crystal sizes increase with increasing

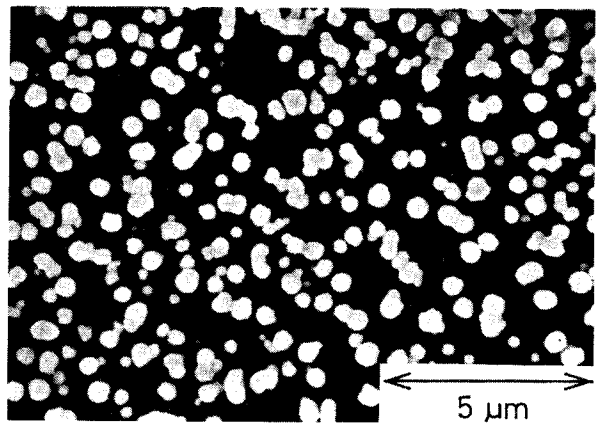

FIG. 2. SEM photograph of Ag crystal peaks formed on a Ag electrode in nonsteady potentiostatic deposition. The surface is horizontal. Deposition time is 10 s, and other data are the same as in Fig. 1.

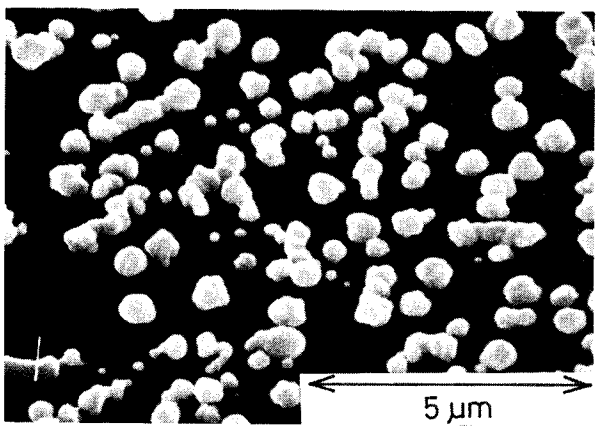

FIG. 1. SEM photograph of Ag crystal peaks formed on a Ag electrode in nonsteady potentiostatic deposition. The surface is slanted upwards at 50°. Applied overpotential is -0.3 V, bulk concentration of $AgClO_4$ in a 10^3 mol m^{-3} $HClO_4$ solution is 56.8 mol m^{-3}, and deposition time is 8.0 s.

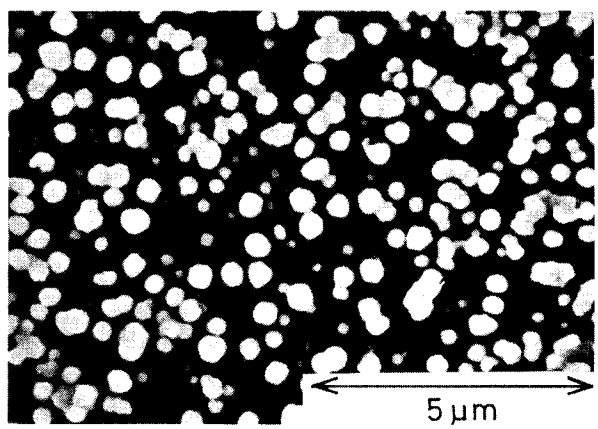

FIG. 3. SEM photograph of Ag crystal peaks formed on a Ag electrode in nonsteady potentiostatic deposition. The surface is horizontal. Deposition time is 20 s, and other data are the same as in Fig. 1.

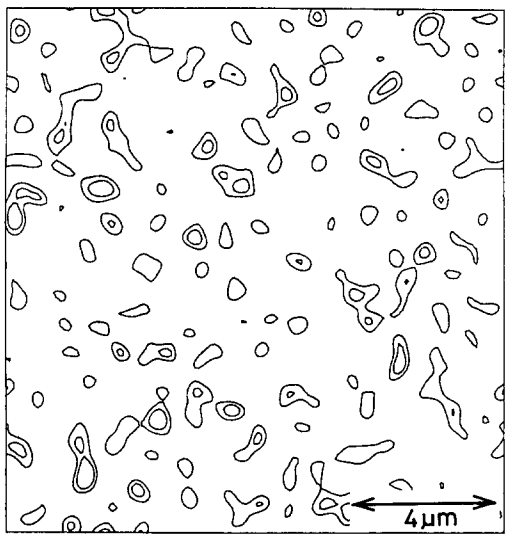

FIG. 4. Theoretical contour line plotting for a silver electrode surface deposited from a Ag ionic solution with a large concentration of supporting electrolyte. Deposition time is 10 s, applied overpotential is -0.3 V and bulk concentration of Ag^+ ion is 56.8 mol m^{-3}. Each contour line is drawn at intervals of the standard deviation of surface height. $D = 1.55\times10^{-9}$ $m^2\,s^{-1}$, $\sigma = 1.7\times10^2$ $\Omega^{-1}\,m^{-1}$, $\Omega = 1.03\times10^{-5}$ $m^3\,mol^{-1}$, $\gamma = 0.55$ $J\,m^{-2}$, $D_{ad} = 1.6\times10^{-10}\,m^2\,s^{-1}$, $C^*_{ad} = 8.0\times10^{-6}$ mol m^{-2}.

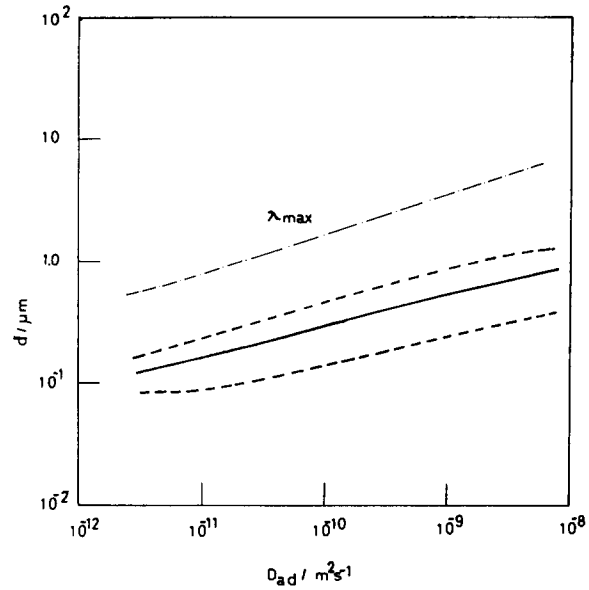

FIG. 6. Dependence of crystal size distribution on the surface diffusion coefficient of Ag adatoms. Bulk concentration of Ag^+ ion 56.8 mol m^{-3}, applied overpotential -0.3 V, deposition time 12.0 s, and other data are the same as in Fig. 4. The solid line is the theoretical average value and the dotted lines depict the theoretical upper and lower error limits.

time, and they have roundish and random shapes without any specific crystal faces. These results seem quite similar to those represented by the theoretical contour line plottings in Figs. 4 and 5. The figures indicate that the crystal sizes increase as the time elapses, and this is also demonstrated by SEM photographs.

Because we did not have the correct values of the surface energy γ and the surface diffusion coefficient, D_{ad} we determined them by adjusting the calculated curves to the experimental data.[11] For this purpose, as shown in Fig. 6, the dependencies of the average size and the standard deviation of the crystal sizes on the surface diffusion coefficient were computed. In the figure, it can be seen that the average size increases with increasing surface diffusion coefficient. Such a large dependence on surface parameters makes it possible to infer reliable values for the matter.

After calculating the relationships between the theoretical crystal size and the deposition time in terms of the

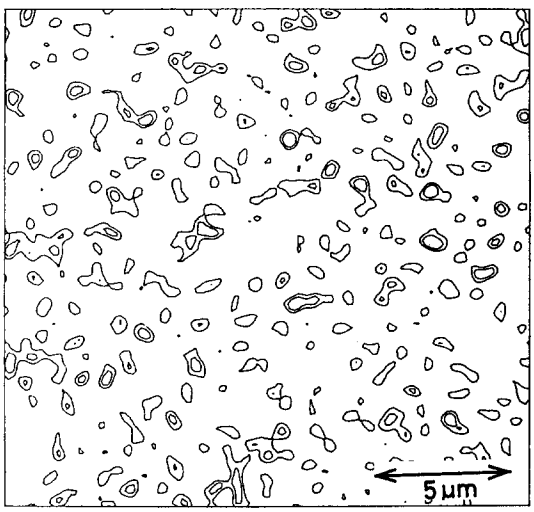

FIG. 5. Theoretical contour line plotting for a silver electrode surface deposited from a Ag ionic solution with a large amount of supporting electrolyte. Bulk concentration of Ag^+ ion 5.68 mol m^{-3}, applied overpotential -0.05 V, surface energy $\gamma = 0.48$ J m^{-2}, deposition time 5.0 s, and other data are the same as in Fig. 4. Each contour line is drawn at intervals of the standard deviation of surface height.

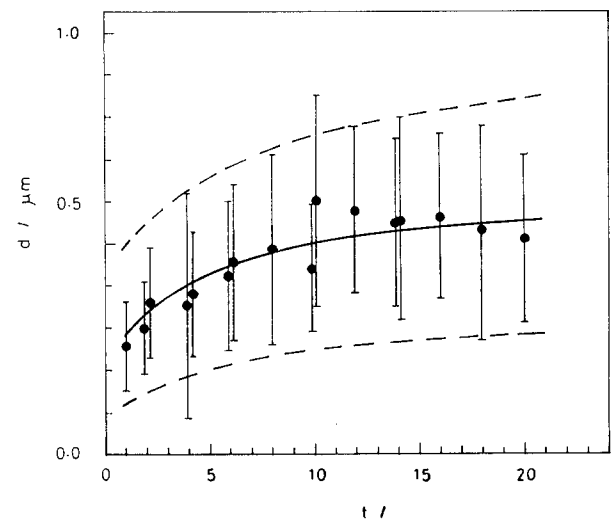

FIG. 7. Crystal size distribution formed on a silver electrode as a function of deposition time. Bulk concentration of Ag^+ ion is 56.8 mol m^{-3}, and applied overpotential is -0.2 V. Solid dots represent the average values of crystal size, and the bars above and below the dots are upper and lower error limits. The solid line is the theoretical average value, and the dotted lines depict the theoretical upper and lower error limits: $D = 1.55\times10^{-9}$ $m^2\,s^{-1}$, $\sigma = 1.7\times10^2$ $\Omega^{-1}\,m^{-1}$, $\Omega = 1.03\times10^{-5}$ $m^3\,mol^{-1}$, $\gamma = 0.55$ $J\,m^{-2}$, $D_{ad} = 1.6\times10^{-10}$ $m^2\,s^{-1}$, $C^*_{ad} = 8.0\times10^{-6}$ mol m^{-2}, and $T = 300$ K.

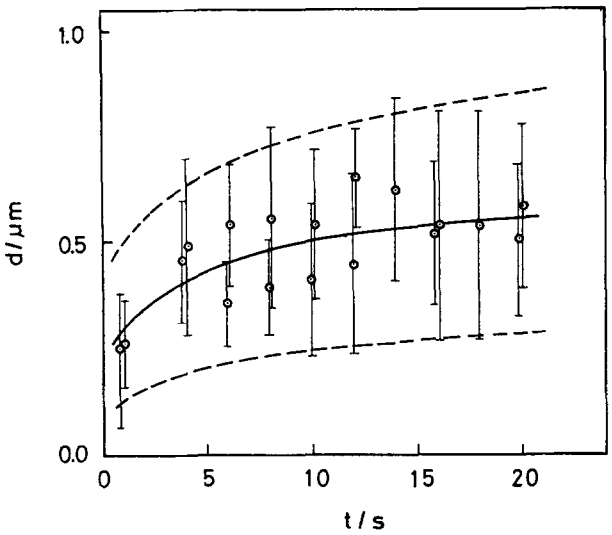

FIG. 8. Variation of silver crystal size formed on a silver electrode with deposition time. Bulk concentration of Ag^+ ion is 56.8 mol m^{-3}, and applied overpotential is -0.3 V. Other data for calculation are the same as in Fig. 7.

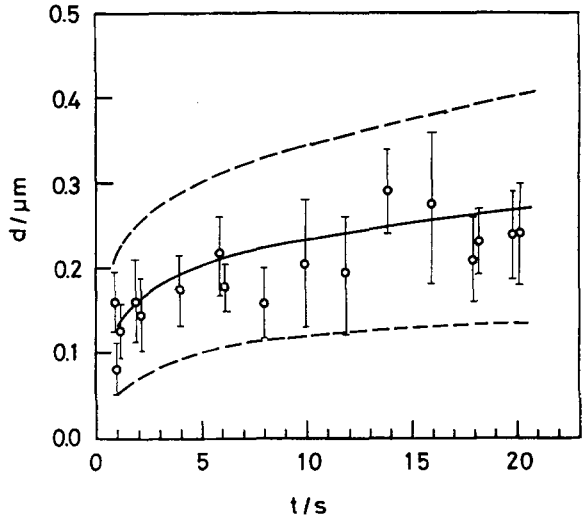

FIG. 10. Variation of silver crystal size formed on a silver electrode with deposition time. Bulk concentration of Ag^+ ion is 5.68 mol m^{-3}, applied overpotential -0.3 V, surface energy $\gamma = 1.9\times10^{-2}$ J m^{-2}, and other data are the same as in Fig. 7.

surface parameters obtained from the procedure mentioned above, the experimental data were compared with them. Figures 7 and 8 are the results calculated and measured for high cathodic overpotentials of -0.2 and -0.3 V. As expected from part I, the figures display that the data both at -0.2 and -0.3 V coincide with each other, i.e., in the high cathodic region, the particle size does not depend on the overpotential. This implies that surface diffusion plays a major role in the deposition process, in particular at higher polarization, and also that the surface energy as well as the surface diffusion coefficient takes a constant value, at least when the potential exceeds about -0.2 V.

If the adatom concentration, C^*_{ad} is assumed to be equal to 8.0×10^{-6} mol m^{-2}, which is established by averaging the data by Bockris *et al.*,[2,3] it can be determined that the surface diffusion coefficient is equal to 1.6×10^{-10} m^2 s^{-1}. This value seems in good agreement with 5×10^{-10} m^2 s^{-1} which is predicted by Bockris *et al.*[12] for Ag electrode surface. As for surface energy, we obtained a constant value: 0.55 J m^{-2} at -0.2 and -0.3 V in the solution with $AgClO_4$ of 56.8 mol m^{-3}.

Then, another experiment was performed under the same conditions mentioned above except for the overpotential -0.05 V and the results are exhibited in Fig. 9. In such region of low overpotential, the average size of the crystals becomes about twice as large as at high overpotential. If the surface diffusion coefficient does not change with overpotential, the surface energy is determined as 1.9 J m^{-2}, which

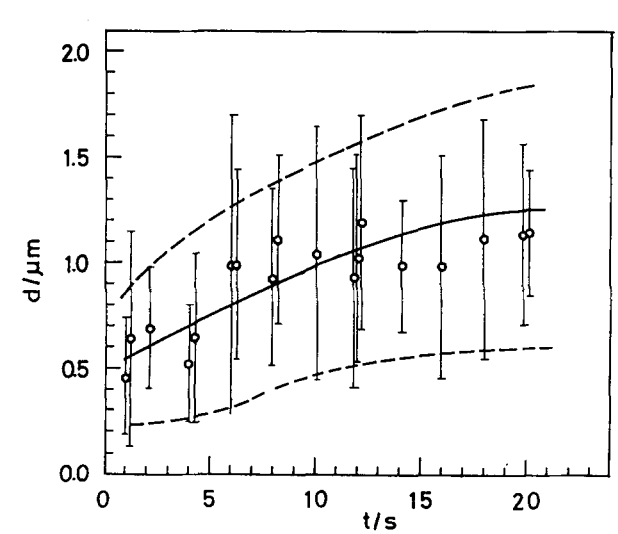

FIG. 9. Variation of silver crystal size formed on a silver electrode with deposition time. Bulk concentration of Ag^+ ion is 56.8 mol m^{-3}, applied overpotential -0.05 V, surface energy $\gamma = 1.9$ J m^{-2}, and other data are the same as in Fig. 7.

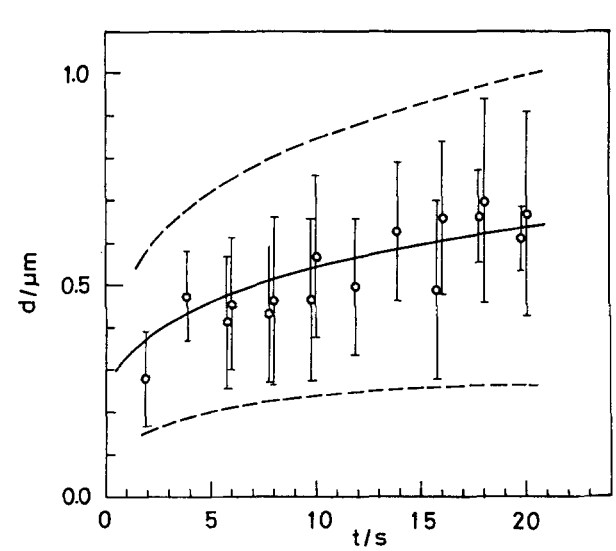

FIG. 11. Variation of silver crystal size formed on a silver electrode with deposition time. Bulk concentration of Ag^+ ion is 5.68 mol m^{-3}, applied overpotential -0.05 V, surface energy $\gamma = 0.48$ J m^{-2}, and other data are the same as in Fig. 7.

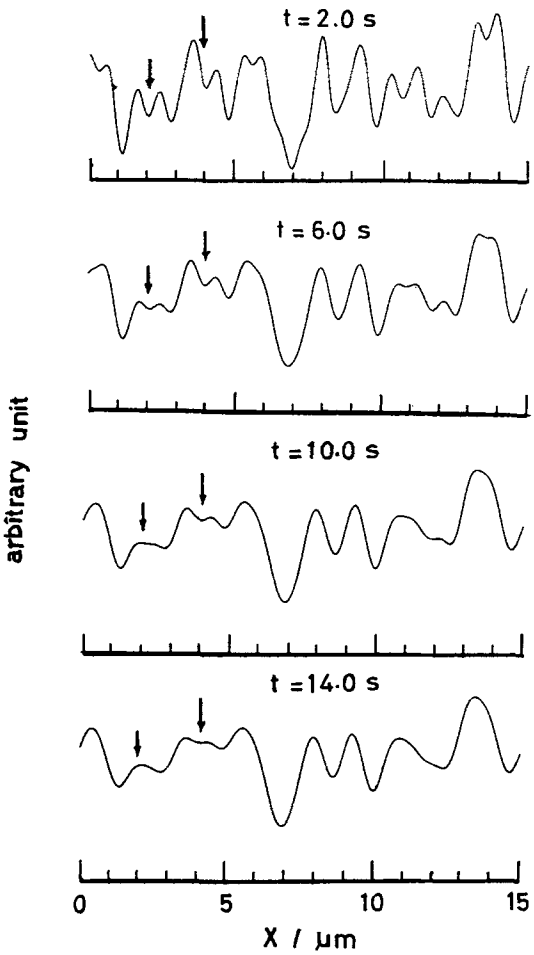

FIG. 12. Time variation in the height of the cross-sectional profile of the silver electrode surface during silver deposition. Bulk concentration of Ag^+ is 56.8 mol m^{-3}, and applied overpotential is -0.3 V. Other data for calculation are the same as in Fig. 4.

leads to the conclusion that the surface energy increases as the overpotential decreases.

Moreover, the surface morphology at the low bulk concentration of 5.68 mol m^{-3} was examined from both aspects of experiments and calculations. Figure 10 represents the dependence of crystal size on the deposition time at the high cathodic overpotential -0.3 V. Comparing these results with those for the case of 56.8 mol m^{-3}, it can be seen that the particle dimensions at the lower concentration become smaller than at the higher concentration. The surface parameters derived from the data are: the surface diffusion coefficient $D_{ad} = 1.6\times10^{-10}$ m^2 s^{-1} and the surface energy $\gamma = 1.9\times10^{-2}$ J m^{-2}. Therefore, it may be concluded that the surface diffusion coefficient is independent of the bulk concentration and the surface energy takes smaller values with decreasing bulk concentration.

Then, the relationship between crystal size and time at the same concentration as in the above case but at different overpotential, -0.05 V is illustrated in Fig. 11. The experimental data and calculations are in good agreement, and Figs. 10 and 11 show the same dependence of crystal size on the overpotential as 56.8 mol m^{-3}, i.e., as the potential decreases, the crystal size increases. In fact, the surface energy $\gamma = 0.48$ J m^{-2}, in the case of -0.05 V, is larger than $\gamma = 1.9\times10^{-2}$ J m^{-2} at -0.3 V.

Finally, in order to examine the time variation of the surface morphology more precisely, typical examples of the calculation were illustrated in the form of cross-sectional profiles. In Fig. 12, all the profiles are made at the same place on the electrode surface. It is found in the figure that as the deposition proceeds, the whole interface of the electrode advances into the solution. In addition, several peaks become incorporated into each other, viz., the crystal peaks formed tend to grow longitudinally. In all cases, however, the vertical growth is scarcely seen, which was obvious from the observation of SEM photographs.

IV. CONCLUSIONS

At high cathodic polarization, it is concluded from the experiments that the distribution of crystal sizes deposited on electrode surface is independent of the overpotential, i.e., the average size and its standard deviation are indifferent to the overpotential. This can be attributed to the fact that surface diffusion strongly affects the mode of crystal growth at high cathodic ranges. At the same time, both the surface diffusion coefficient and surface energy are concluded to be constant, at least, in the most cathodic region.

However, at lower cathodic potentials, it was found that the surface energy increases with decreasing overpotential. From SEM observations, the crystal sizes have a tendency to increase with decreasing bulk concentration. The latter experimental result presents the conclusion that the surface energy decreases as the concentration decreases.

Furthermore, the cross-sectional profiles simulating an electrode surface during the crystal formation made it clear that the concave parts of the surface are preferably filled up until larger crystal peaks emerge.

ACKNOWLEDGMENTS

The authors wish to thank Professor S. Yamauchi of the University of Tokyo for displaying the results of calculations by computer graphics. The discussion with him was quite helpful in establishing some of the results explained here. Publication costs of this article were assisted by the Institute of Vocational Training.

[1] A. Damjanović and J. O'M. Bockris, J. Electrochem. Soc. **110**, 1035 (1963).
[2] W. Mehl and J. O'M. Bockris, Can. J. Chem. **37**, 190 (1959).
[3] W. Mehl and J. O'M. Bockris, J. Chem. Phys. **27**, 817 (1957).
[4] A. R. Despić and J. O'M. Bockris J. Chem. Phys. **32**, 389 (1960).
[5] H. Gerischer, Z. Elektrochem. **62**, 256 (1958).
[6] W. Lorenz, Z. Phys. Chem. **19**, 377 (1959).
[7] M. Fleischmann and H. R. Thirsk, Electrochim. Acta **2**, 22 (1960).
[8] T. R. Beck, J. Phys. Chem. **73**, 466 (1969).
[9] R. Aogaki, J. Electrochem. Soc. **129**, 2442 (1982).
[10] R. Aogaki, J. Electrochem. Soc. **129**, 2447 (1982).
[11] T. Makino and R. Aogaki, Denki Kagaku **51**, 289 (1983).
[12] J. O. M. Bockris and G. A. Razumney, in *Fundamental Aspects of Electrocrystallization* (Plenum, New York, 1967), p. 64.
[13] E. O. Brigham, *The Fast Fourier Transform* (Prentice-Hall, Englewood Cliffs, 1974).
[14] R. Aogaki and T. Makino, J. Electrochem. Soc. **131**, 47 (1984).